第 24 卷第 2 期 无 机 化 学 学 报 Vol.24 No.2
2008 年 2 月 CHINESE JOURNAL OF INORGANIC CHEMISTRY 246~252

纳米结晶体 $Ni_{0.5}Zn_{0.5}Fe_2O_4$ 对高氯酸铵热行为及分解反应动力学的影响

仪建华[1] 赵凤起*,[1] 胡荣祖[1] Gurdip Singh[2]
([1]西安近代化学研究所,西安 710065)
([2]DDU Gorakhpur 大学化学系,Gorakhpur 273009,印度)

摘要:采用差示扫描量热法(DSC)、热重和微分热重(TG-DTG)及固相原位反应池/快速扫描傅立叶变换红外联用技术(hyphenated *in situ* thermolysis/RSFTIR)研究了纳米结晶体 $Ni_{0.5}Zn_{0.5}Fe_2O_4$ 与高氯酸铵(AP)组成的混合物的热行为和分解反应动力学。结果表明:$Ni_{0.5}Zn_{0.5}Fe_2O_4$ 使得 AP 的低、高温分解放热峰温分别提前 17.44 K 和 27.74 K,并使得对应的分解热分别增加 3.7 $J\cdot g^{-1}$ 和 193.7 $J\cdot g^{-1}$。$Ni_{0.5}Zn_{0.5}Fe_2O_4$ 并不影响 AP 的晶转温度和晶转热。$Ni_{0.5}Zn_{0.5}Fe_2O_4$ 使得 AP 的 TG 曲线出现 3 个阶段,并使得后 2 个失重阶段的初始和终止温度都有所提前。凝聚相分解产物分析表明 $Ni_{0.5}Zn_{0.5}Fe_2O_4$ 加速了凝聚相 AP 的分解及氨气的释放。含 $Ni_{0.5}Zn_{0.5}Fe_2O_4$ 的 AP 的高温分解反应的动力学参数 E_a=238.88 $kJ\cdot mol^{-1}$,$A=10^{18.59}$ s^{-1},动力学方程可表示为 $d\alpha/dt=10^{18.99}(1-\alpha)[-\ln(1-\alpha)]^{3/5}e^{-2.87\times10^4/T}$。始点温度($T_e$)和峰顶温度($T_p$)计算得出 AP 的热爆炸临界温度值分别为:574.83 K 和 595.41 K。分解反应的活化熵($\Delta S^{\neq}$)、活化焓($\Delta H^{\neq}$)和活化能($\Delta G^{\neq}$)分别为:109.61 $J\cdot mol^{-1}\cdot K^{-1}$、236.49 $kJ\cdot mol^{-1}$ 及 172.58 $kJ\cdot mol^{-1}$。

关键词:纳米结晶体;$Ni_{0.5}Zn_{0.5}Fe_2O_4$;高氯酸铵(AP);热行为;非等温反应动力学
中图分类号:O643 **文献标识码**:A **文章编号**:1001-4861(2008)02-0246-07

Effect of Nanocrystal $Ni_{0.5}Zn_{0.5}Fe_2O_4$ on Thermal Behavior and Decomposition Reaction Kinetics of Ammonium Perchlorate

YI Jian-Hua[1] ZHAO Feng-Qi*,[1] HU Rong-Zu[1] Gurdip Singh[2]
([1]*Xi'an Modern Chemistry Research Institute, Xi'an* 710065)
([2]*Chemistry Department, DDU Gorakhpur University, Gorakhpur* 273009, *India*)

Abstract: The thermal behavior and non-isothermal decomposition reaction kinetics of the mixture of the nanocrystal $Ni_{0.5}Zn_{0.5}Fe_2O_4$ and ammonium perchlorate (AP) were investigated by differential scanning calorimetry (DSC), thermogravimetry and differential thermogravimetry (TG-DTG), and the hyphenated technique of *in situ* thermolysis cell with rapid-scan Fourier transform infrared spectroscopy (in situ thermolysis/RSFTIR). The results show that $Ni_{0.5}Zn_{0.5}Fe_2O_4$ can decrease the low-temperature and the high-temperature exothermic peak temperatures of AP by 17.44 K and 27.74 K, respecti vely, and increase the decomposition heats of the two exothermic peaks by 3.7 $J\cdot g^{-1}$ and 193.7 $J\cdot g^{-1}$, respectively. $Ni_{0.5}Zn_{0.5}Fe_2O_4$ does not affect the crystal transformation temperature and heat of AP. $Ni_{0.5}Zn_{0.5}Fe_2O_4$ makes AP shown three mass-loss processes, and it can decrease the initial and terminated temperatures of the last two mass-loss stages. The condensed phase decomposition product analysis shows that $Ni_{0.5}Zn_{0.5}Fe_2O_4$ accelerates the decomposition of condensed AP and the release of the gaseous NH_3. The kinetic parameters E_a=238.88 $kJ\cdot mol^{-1}$, $A=10^{18.59}s^{-1}$, and the kinetic equation of the high-temperature decomposition reaction of $Ni_{0.5}Zn_{0.5}Fe_2O_4$/AP can be described as: $d\alpha/dt=10^{18.99}(1-\alpha)[-\ln(1-\alpha)]^{3/5}e^{-2.87\times10^4/T}$. The corresponding critical

收稿日期:2007-10-10。收修改稿日期:2007-11-16。
国家自然科学基金(No.20573098)和火炸药燃烧国防科技重点实验室基金(No.9140C3503020605)资助项目。
*通讯联系人。E-mail:npecc@21cn.com;yiren@nwu.edu.cn
第一作者:仪建华,男,31 岁,工程师,博士研究生;研究方向:含能材料的热分解机理及动力学。

temperatures of thermal explosion (T_{be} and T_{bp}) corresponding to $\beta \to 0$ are 574.83 K and 595.41 K, respectively. The entropy of activation ($\Delta S^{\neq}$), enthalpy of activation ($\Delta H^{\neq}$), and free energy of activation ($\Delta G^{\neq}$) of the decomposition reaction are 109.61 J·mol^{-1}·K^{-1}, 236.49 kJ·mol^{-1}, and 172.58 kJ·mol^{-1}, respectively.

Key words: Nanocrystal; $Ni_{0.5}Zn_{0.5}Fe_2O_4$; ammonium perchlorate (AP); thermal behavior; non-isothermal reaction kinetics

Ammonium perchlorate (AP) is one of the main oxidants in solid composite propellants in common use, and its thermal decomposition has a large effect on the combustion of the solid propellants. Scientists have developed extensive research works on the thermal decomposition of AP in recent years[1~5]. They had various opinions on the catalyzed decomposition processes of AP, and considered that different catalysts had different effects on the decomposition processes of AP. Many literatures appeared on the thermal decomposition of AP influenced by metal powder and metal oxides[6~11]. Ferrite used as magnetite appeared frequently[12,13], but the catalytic activity on the decomposition of AP has not been reported in public to the best of our knowledge. In this paper, the effect of the nanocrystal $Ni_{0.5}Zn_{0.5}Fe_2O_4$ on the thermal behavior and decomposition reaction kinetics of AP are discussed.

1 Experimental

1.1 Sample

AP (100 μm ~150 μm) was ground with the nanocrystal $Ni_{0.5}Zn_{0.5}Fe_2O_4$ (0.80 μm ~1 μm) by 1% (mass fraction) in an agate mortar to prepare the sample for the thermal decomposition experiment. AP was of propellant grade and used without further purification or additives. The nanocrystal $Ni_{0.5}Zn_{0.5}Fe_2O_4$ was prepared according to the previous method[12].

1.2 Equipment and conditions

The DSC and TG-DTG curves under the condition of flowing nitrogen gas (purity, 99.999%) were obtained by using a 204HP differential scanning calorimeter (Netzsch Co., Germany) and a TA2950 thermal analyzer (TA Co., USA), respectively. The conditions of DSC analyses were: N_2 flowing rate, 50 cm^3·min^{-1}; heating rate, 10 K·min^{-1}; sample mass, about 1 mg; pressure, 0.1 MPa; reference sample, α-Al_2O_3. The conditions of TG-DTG were as follows: N_2 flowing rate, 40 cm^3·min^{-1}; heating rate (β), 10 K·min^{-1}; sample mass, about 1 mg. The non-isothermal DTG analyses were studied at the heating rates of 5, 10, and 15 K·min^{-1}.

The hyphenated technique of *in situ* thermolysis cell (Amoy University Instrument Co., China) with rapid-scan Fourier transform infrared spectroscopy (Nicolet 60SXR, Nicolet Co., USA) (*in situ* thermolysis/RSFTIR) was employed to explore the thermal decomposition process. The thermolysis cell heating rate, 10 K·min^{-1}; atmosphere, air. Solid thermolysis spectra acquisition rate, 7.48 files·min^{-1}; resolution, 4 cm^{-1}; a DTGS detector.

2 Results and discussion

2.1 Thermal behaviors

The DSC and TG-DTG curves at a heating rate of 10 K·min^{-1} for $Ni_{0.5}Zn_{0.5}Fe_2O_4$/AP and AP are shown in Figs.1 and 2, respectively. From Fig.1, one can see that there are one endothermic peak and two exothermic peaks in one of the DSC curves. $Ni_{0.5}Zn_{0.5}Fe_2O_4$ can decrease the low-temperature and the high-temperature exothermic peak temperatures of AP by 17.44 K and 27.74 K, respectively. $Ni_{0.5}Zn_{0.5}Fe_2O_4$ can increase the decomposition heats of the two exothermic peaks from 139.4 J·g^{-1} to 143.1 J·g^{-1} and 579.2 J·g^{-1} to 772.9 J·g^{-1},

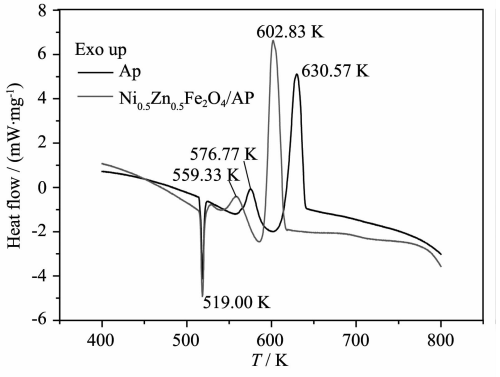

Fig.1 DSC curves for AP and $Ni_{0.5}Zn_{0.5}Fe_2O_4$/AP at a heating rate of 10 K·min^{-1}

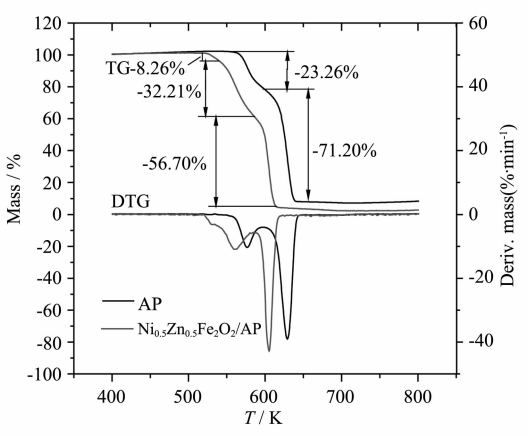

Fig.2 TG-DTG curves for AP and $Ni_{0.5}Zn_{0.5}Fe_2O_4$/AP at a heating rate of 10 K·min^{-1}

respectively. The crystal transformation temperature of AP is not affected by $Ni_{0.5}Zn_{0.5}Fe_2O_4$, and the heat absorption keeps at 76.7 J·g^{-1}.

From Fig.2, one can see that $Ni_{0.5}Zn_{0.5}Fe_2O_4$ makes AP shown three mass-loss processes, and it can decrease the initial temperatures of the last two mass-loss processes from 559.63 K to 516.02 K and 598.17 K to 586.11 K, respectively. The third mass-loss processes of $Ni_{0.5}Zn_{0.5}Fe_2O_4$/AP and AP terminate at 618.20 K and 643.17 K, and leave the residue of 3.83% and 5.54% (mass fraction), respectively.

The IR absorption spectra of the *in situ* condensed phase thermolysis products of $Ni_{0.5}Zn_{0.5}Fe_2O_4$/AP at various temperatures and the curves of characteristic band intensity as a function of the temperature are shown in Figs.3 and 4, respectively, and those of AP are shown in Figs.5 and 6, respectively. It can be clearly seen that the spectra intensity of ClO_4^- [1 100~1 025 cm^{-1}(s), 650 ~600 cm^{-1}(s)] and NH_4^+ [3 300~3 030 cm^{-1} (vs), 1 430~1 390 cm^{-1} (s)] of $Ni_{0.5}Zn_{0.5}Fe_2O_4$/AP are

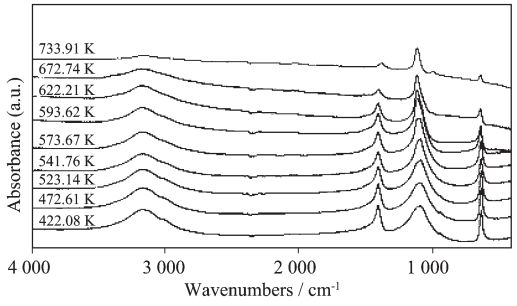

Fig.3 IR spectra of the condensed phase decomposition products of $Ni_{0.5}Zn_{0.5}Fe_2O_4$/AP at various temperatures

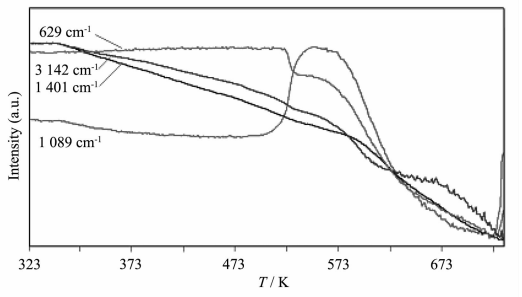

Fig.4 IR characteristic absorption peak intensity of the condensed phase decomposition products of $Ni_{0.5}Zn_{0.5}Fe_2O_4$/AP at various temperatures

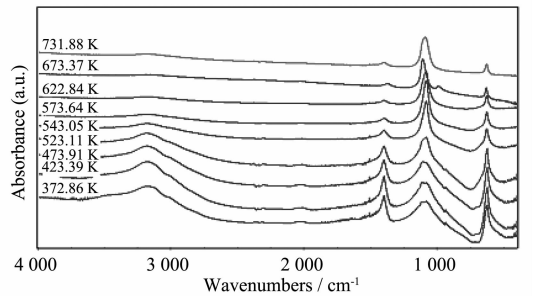

Fig.5 IR spectra of the condensed phase decomposition products of AP at various temperatures

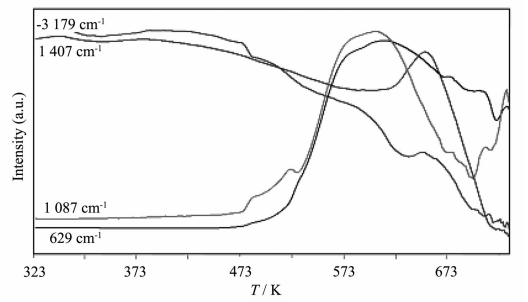

Fig.6 IR characteristic absorption peak intensity of the condensed phase decomposition products of AP at various temperatures

different from AP, and $Ni_{0.5}Zn_{0.5}Fe_2O_4$ changes the thermal decomposition processes of AP. With the rising of temperature, the spectra intensity of NH in the condensed phase of $Ni_{0.5}Zn_{0.5}Fe_2O_4$/AP rapid falls down, while that of AP keeps the same till about 470 K, then shows a falling trend, and the spectra intensity of ClO in the condensed phase of AP rises at first, and falls down from 600 K which corresponds to the high-temperature exothermic peak temperature. Therefore, it can be concluded that $Ni_{0.5}Zn_{0.5}Fe_2O_4$ accelerates the decomposition of condensed AP and the release of the gaseous NH_3.

2.2 Calculation of non-isothermal reaction kinetics

To explore the thermal decomposition mechanism of the high-temperature decomposition process (the third mass-loss stage) of AP containing $Ni_{0.5}Zn_{0.5}Fe_2O_4$ and obtain the corresponding kinetic parameters [apparent activation energy (E_a/(kJ·mol^{-1})), preexponential constant (A/s^{-1})] and the most probable kinetic model function, the DTG curves at heating rates of 5, 10, and 15 K·min^{-1} were dealt with mathematic means, and five integral methods [Eqs. (**1**) ~(**5**)] and one differential methods [Eq. (**6**)] listed in Table 1 are employed [14-24].

In these equations, α is the conversion degree of stage Ⅲ; T, the temperature (K) at time of t; T_e and T_p are the onset temperature and the peak temperature of the DTG curve, respectively; R, the gas constant; $f(\alpha)$ and $G(\alpha)$ are the differential model function and the integral model function, respectively, and E_a, A, and β have been defined above. The data needed for the equations of the integral and differential methods, α_i, β, T_i, T_e, and T_p, are obtained from the DTG curves and summarized in Table 2.

Table 1　Kinetic analysis methods

Method	Equation	
Ordinary-integral	$\ln\frac{G(\alpha)}{T^2}=\ln\left[\frac{AR}{\beta E}\left(1-\frac{2RT}{E}\right)\right]-\frac{E}{RT}$	(**1**)
Mac Callum-Tanner	$\lg G(\alpha)=\lg\frac{AE}{\beta R}-0.482\,8\,E^{0.435\,7}-\frac{0.449+0.217E}{0.001T}$　(E in kcal·mol^{-1})	(**2**)
Šatava-Šesták	$\lg G(\alpha)=\lg\frac{A_S E_S}{\beta R}-2.315-0.456\,7\frac{E_S}{RT}$	(**3**)
Agrawal	$\ln\frac{G(\alpha)}{T^2}=\ln\frac{\frac{AR}{\beta E}\left(1-2\frac{RT}{E}\right)}{1-5\left(\frac{RT}{E}\right)^2}-\frac{E}{RT}$	(**4**)
Flynn-Wall-Ozawa	$\lg\beta=\lg\frac{AE}{RG(\alpha)}-2.315-0.456\,7\frac{E}{RT}$	(**5**)
Kissinger	$\ln\frac{\beta_i}{T_{pi}^2}=\ln\frac{A_k R}{E_k}-\frac{E_k}{RT_{pi}}$　i=1,2,3,4	(**6**)

Table 2　Basic data for the high-temperature decomposition process of $Ni_{0.5}Zn_{0.5}Fe_2O_4$/AP

α	T / K			α	T / K			α	T / K		
	5 K·min^{-1}	10 K·min^{-1}	15 K·min^{-1}		5 K·min^{-1}	10 K·min^{-1}	15 K·min^{-1}		5 K·min^{-1}	10 K·min^{-1}	15 K·min^{-1}
0.01	585.58	592.60	595.18	0.35	597.61	607.10	609.56	0.69	602.37	611.96	614.31
0.02	586.28	593.58	596.22	0.36	597.77	607.26	609.71	0.70	602.52	612.11	614.46
0.03	587.11	594.54	597.21	0.37	597.93	607.42	609.86	0.71	602.67	612.26	614.62
0.04	587.91	595.44	598.15	0.38	598.08	607.58	610.00	0.72	602.82	612.41	614.78
0.05	588.68	596.30	599.05	0.39	598.23	607.73	610.15	0.73	602.98	612.56	614.95
0.06	589.38	597.07	599.89	0.40	598.37	607.88	610.29	0.74	603.14	612.71	615.12
0.07	589.98	597.82	600.66	0.41	598.52	608.03	610.43	0.75	603.30	612.87	615.29
0.08	590.53	598.55	601.38	0.42	598.66	608.18	610.56	0.76	603.47	613.02	615.47
0.09	591.05	599.24	602.02	0.43	598.81	608.32	610.70	0.77	603.64	613.17	615.64
0.10	591.52	599.88	602.62	0.44	598.95	608.47	610.84	0.78	603.81	613.33	615.83
0.11	591.95	600.47	603.17	0.45	599.09	608.61	610.97	0.79	603.99	613.49	616.02
0.12	592.35	601.02	603.68	0.46	599.23	608.75	611.10	0.80	604.16	613.65	616.21
0.13	592.72	601.53	604.14	0.47	599.37	608.89	611.24	0.81	604.35	613.81	616.41
0.14	593.06	601.99	604.57	0.48	599.50	609.03	611.37	0.82	604.53	613.97	616.61
0.15	593.36	602.41	604.97	0.49	599.64	609.17	611.51	0.83	604.72	614.14	616.83

Continued Table 2

0.16	593.67	602.79	605.33	0.50	599.78	609.31	611.65	0.84	604.91	614.31	617.05
0.17	593.96	603.15	605.68	0.51	599.91	609.44	611.78	0.85	605.11	614.48	617.27
0.18	594.24	603.48	606.00	0.52	600.04	609.58	611.92	0.86	605.31	614.65	617.51
0.19	594.50	603.79	606.30	0.53	600.18	609.72	612.05	0.87	605.52	614.84	617.76
0.20	594.76	604.07	606.59	0.54	600.31	609.86	612.19	0.88	605.74	615.02	618.02
0.21	595.00	604.34	606.85	0.55	600.45	610.00	612.32	0.89	605.97	615.21	618.29
0.22	595.23	604.59	607.11	0.56	600.58	610.13	612.45	0.90	606.21	615.40	618.57
0.23	595.45	604.83	607.34	0.57	600.72	610.27	612.59	0.91	606.47	615.60	618.87
0.24	595.67	605.06	607.58	0.58	600.85	610.41	612.72	0.92	606.75	615.81	619.18
0.25	595.88	605.27	607.79	0.59	600.99	610.55	612.86	0.93	607.04	616.02	619.53
0.26	596.07	605.48	608.00	0.60	601.12	610.69	613.00	0.94	607.37	616.24	619.91
0.27	596.25	605.67	608.20	0.61	601.26	610.83	613.14	0.95	607.74	616.49	620.33
0.28	596.42	605.87	608.38	0.62	601.39	610.97	613.28	0.96	608.19	616.76	620.83
0.29	596.61	606.06	608.57	0.63	601.53	611.11	613.42	0.97	608.76	617.08	621.45
0.30	596.78	606.24	608.75	0.64	601.66	611.25	613.56	0.98	609.49	617.51	622.25
0.31	596.95	606.43	608.92	0.65	601.80	611.39	613.70	0.99	610.22	618.33	623.55
0.32	597.13	606.60	609.09	0.66	601.94	611.53	613.85	1.00	615.21	623.12	629.14
0.33	597.29	606.77	609.25	0.67	602.08	611.67	614.00		T_e=584.45 K	T_e=596.26 K	T_e=598.77 K
0.34	597.45	606.94	609.40	0.68	602.23	611.82	614.15		T_p=600.39 K	T_p=610.36 K	T_p=612.99 K

The values of E_a were obtained by Ozawa′s method [Eq.(**5**)] with changing from 0.01 to 1.00 as shown in Table 2, and the E_a-α curve is shown in Fig.7. From Fig.7, one can see that activation energy changes significantly with the increase of conversion degree except for the section of 0.05~0.95 (α). In this section, activation energy changes faintly, which means that the decomposition mechanism of the process does not transfer in essence or the transference could be ignored. So, it is feasible to study the reaction mechanism and kinetics in this section.

Forty-one types of kinetic model functions in Ref.[19] and the original data tabulated in Table 2 are put into Eqs. (**1**) ~(**6**) respectively for calculations. The values of E_a, lg$A$, linear correlation coefficient (r) and standard mean square deviation (Q) can be calculated

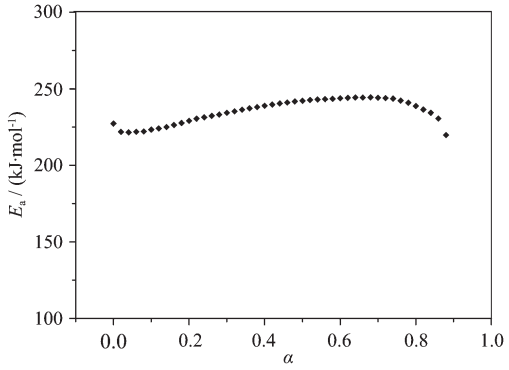

Fig.7 E_a-α curve obtained by Ozawás method

Table 3 Kinetic parameters obtained for the high-temperature decomposition process of $Ni_{0.5}Zn_{0.5}Fe_2O_4$/AP

Method	β / (K·min^{-1})	E_a / (kJ·mol^{-1})	lg(A / s^{-1})	r	Q
Ordinary-integral	5	242.90	18.93	0.998 2	0.044 8
	10	237.18	18.39	0.999 4	0.016 0
	15	235.76	18.36	0.998 1	0.049 3
Mac Callum-Tanner	5	246.00	19.25	0.998 4	0.008 4
	10	240.38	18.71	0.999 4	0.003 0
	15	239.00	18.68	0.998 2	0.009 3
Šatava-Šesták	5	240.45	18.72	0.998 4	0.008 4
	10	235.15	18.22	0.999 5	0.003 0
	15	233.84	18.19	0.998 2	0.009 3

Continued Table 3

Agrawal	5	242.90	18.93	0.998 2	0.044 8
	10	237.18	18.39	0.999 4	0.016 0
	15	235.76	18.36	0.998 1	0.049 3
Mean		238.88	18.59		
Flynn-Wall-Ozawa		239.09		0.984 2	0.003 6
Kissinger		241.34	18.81	0.982 9	0.019 3

by the computer with the linear least-squares method at various heating rates of 5, 10, and 15 $K \cdot min^{-1}$. The most probable mechanism function is selected by the better values of r, and Q taken from[19,21~24]. The results satisfying the above-mentioned conditions at the same time are the final results as listed in Table 3, and the relevant function is the reaction mechanism function of the high-temperature decomposition process of AP containing $Ni_{0.5}Zn_{0.5}Fe_2O_4$.

The data in Table 3 indicate that the values of E_a and lg$A$ obtained by Eqs.(**1**)~(**4**) are approximately in agreement with the values calculated by Ozawa′s method and Kissinger′s method. Therefore, the reaction mechanism of the high-temperature decomposition process of $Ni_{0.5}Zn_{0.5}Fe_2O_4$/AP can be classified as nucleation and growth, and the corresponding Avrami-Erofeev equation (n =2/5) controls the decomposition process. The mechanism function $G(\alpha)=[-\ln(1-\alpha)]^{2/5}$, $f(\alpha)=(5/2)(1-\alpha)[-\ln(1-\alpha)]^{3/5}$. Substituting $f(\alpha)$ with $(5/2)(1-\alpha)[-\ln(1-\alpha)]^{3/5}$, E_a/(kJ·mol^{-1}) with 238.88 and A/s^{-1} with $10^{18.59}$ into Eq.(**7**):

$$d\alpha/dt = A\, f(\alpha) e^{-E/RT} \quad (7)$$

the kinetic equation of the high-temperature decomposition reaction of $Ni_{0.5}Zn_{0.5}Fe_2O_4$/AP can be described as:

$$d\alpha/dt = 10^{18.99}(1-\alpha)[-\ln(1-\alpha)]^{3/5} e^{-2.87\times10^4 T}$$

The values (T_{e0} and T_{p0}) of the onset temperature (T_e) and peak temperature (T_p) corresponding to $\beta \to 0$ obtained by Eq.(**8**) taken from[19,21~24] are 563.34 K and 583.08 K, respectively.

$$T_{ei\ or\ pi} = T_{e0\ or\ p0} + b\beta_i + c\beta_i^2 \quad i = 1\sim3 \quad (8)$$

where b and c are coefficients.

The corresponding critical temperatures of thermal explosion (T_{be} and T_{bp}) obtained from Eq.(**9**) taken from[19,21~24] are 574.83 K and 595.41 K, respectively.

$$T_{be\ or\ bp} = \left(E_O - \sqrt{E_O^2 - 4E_O R T_{e0\ or\ p0}}\right)/(2R) \quad (9)$$

where R is the gas constant (8.314 J·mol^{-1}·K^{-1}), and E_O the value of E_a calculated by Ozawa′s method.

The entropy of activation ($\Delta S^{\neq}$), enthalpy of activation ($\Delta H^{\neq}$), and free energy of activation ($\Delta G^{\neq}$) of the decomposition reaction, corresponding to $T=T_{p0}$, $E_a=E_k$, and $A=A_k$, obtained from Eqs.(**10**)~(**12**)[15~18] are 109.61 J·mol^{-1}·K^{-1}, 236.49 kJ·mol^{-1}, and 172.58 kJ·mol^{-1}, respectively.

$$A = (k_B T/h)\, e^{\Delta S^{\neq}/R} \quad (10)$$

$$\Delta H^{\neq} = E_a - RT \quad (11)$$

$$\Delta G^{\neq} = \Delta H^{\neq} - T\Delta S^{\neq} \quad (12)$$

where k_B is the Boltzmann constant (1.380 7×10^{-23} J·K^{-1}), and h is the Plank constant (6.626×10^{-34} J·s).

3 Summary

$Ni_{0.5}Zn_{0.5}Fe_2O_4$ can decrease the low-temperature and the high-temperature exothermic peak temperatures of AP and increase the decomposition heats of the two exothermic peaks. $Ni_{0.5}Zn_{0.5}Fe_2O_4$ does not affect the crystal transformation temperature and heat of AP. $Ni_{0.5}Zn_{0.5}Fe_2O_4$ makes AP shown three mass-loss stages, and decreases the initial and terminated temperatures of the last two mass-loss processes. $Ni_{0.5}Zn_{0.5}Fe_2O_4$ accelerates the decomposition of condensed AP and the release of the gaseous NH_3. The kinetic parameters E_a= 238.88 kJ·mol^{-1}, $A=10^{18.59}$ s^{-1}, and the kinetic equation of the high-temperature decomposition reaction of $Ni_{0.5}Zn_{0.5}Fe_2O_4$/AP can be described as: $d\alpha/dt = 10^{18.99}(1-\alpha)[-\ln(1-\alpha)]^{3/5} e^{-2.87\times10^4 T}$. The corresponding critical temp-eratures of thermal explosion (T_{be} and T_{bp}) corresponding to $\beta \to 0$ are 574.83 K and 595.41 K, respectively. ΔS, ΔH, and ΔG of the decomposition

reaction are 109.61 $J \cdot mol^{-1} \cdot K^{-1}$, 236.49 $kJ \cdot mol^{-1}$, and 172.58 $kJ \cdot mol^{-1}$, respectively.

References:

[1] Shadman Y F. *AD* 746728, 1972.

[2] Pearson G S. *Combust. Sci. Techno*., **1971**,**3**(4):155~163

[3] Brill T B, Brush P J, Patil D G. *Combustion and Flame*, **1993**, **94**:70~76

[4] MA Zhen-Ye(马振叶), LI Feng-Sheng(李凤生), CUI Ping (崔 平), et al. *Chin. J. Catal.* (*Cuihua Xuebao*), **2003**,**24**(10): 795~798

[5] LIU Zi-Ru(刘子如), YIN Cui-Mei(阴翠梅), KONG Yang-Hui (孔扬辉), et al. *Chin. J. Ener. Mater.* (*Hanneng Cailiao*), **2000**, **8**(2):75~79

[6] LI Shu-Fen(李疏芬), JIANG Zhi(江 治), ZHAO Feng-Qi (赵凤起), et al. *Chin. J. Chem. Phys.* (*Huaxue Wuli Xuebao*), **2004**,**17**(5):623~628

[7] Survase D V, Gupta M, Asthana S N. *Progress in Crystal Growth and Characterization*, **2002**,**45**,161~165

[8] DUAN Guo-Rong(段国荣), YANG Xu-Jie(杨绪杰), CHEN Jian(陈 建), et al. *Powder Techno.*, **2007**,**172**:27~29

[9] Said A A, Aloasmi R. *Thermochimica Acta*, **1996**,**275**(1):83

[10]LIU Lei-Li(刘磊力), LI Feng-Sheng(李凤生), YANG Yi (杨 毅), et al. *Chinese J. Inorg. Chem.* (*Wuji Huaxue Xuebao*), **2005**,**21**(10):1525~1530

[11]LUO Yuan-Xiang(罗元香), LU Lu-De(陆路德), LIU Xiao-Heng(刘孝恒), et al. *Chinese J. Inorg. Chem.* (*Wuji Huaxue Xuebao*), **2002**,**18**(12):1211~1214

[12]ZHU Wei-Chang(朱伟长), ZHANG Dong-Sheng(张东生), PAN Feng(潘 峰). *J. Southeast U.* (*Natur. Sci. Ed.*)(*Dongnan Daxue Xuebao* (*Ziran Kexue Ban*)), **2003**,**33**(2):241~244

[13]LI Yao(李 垚), ZHAO Jiu-Peng(赵九蓬), HAN Jie-Cai (韩杰才), et al. *J. Chinese Ceram. Soc.*(*Guisuanyan Xuebao*), **2000**,**28**(5): 427~431

[14]Mac Callum J R. Tanner *J. Eur. Polymer J.*, **1968**,**4**:333

[15]Šatava V, Šesták J. *J. Them. Anal.*, **1975**,**8**(3):477~489

[16]Agrawal R K. *J. Therm. Anal.*, **1987**,**32**(1):149~156

[17]Kissinger H E. *Anal. Chem*., **1957**,**29**(11):1702~1706

[18]Ozawa T. *Bull. Chem. Soc. Jpn.*, **1965**,**38**(11):1881~1886

[19]HU Rong-Zu(胡荣祖), SHI Qi-Zheng(史启祯). *Thermal Analysis Kinetics*(热分析动力学). Beijing: Science Press, **2001.**

[20]SONG Xiu-Duo(宋秀铎), ZHAO Feng-Qi(赵凤起), LIU Zi-Ru(刘子如), et al. *Chem. J. Chin. Univ.*(*Gaodeng Xuexiao Huexue Xuebao*), **2006**,**27**:125~128

[21]ZHANG Tong-Lai(张同来). *Thesis for the Doctorate of Nanjing University of Science & Technology*(南京理工大学博士论文). **1993**.

[22]MA Hai-Xia(马海霞), SONG Ji-Rong(宋纪蓉), HU Rong-Zu (胡荣祖). *Chin. J. Chem.*(*Zhongguo Huexue*), **2003**,**21**:1558 ~1561

[23]HU Rong-Zu(胡荣祖), CHEN San-Ping(陈三平), GAO Sheng-Li(高胜利). *J. Hazard. Mater.*, **2005**,**A117**:103~110

[24]YI Jian-Hua(仪建华), ZHAO Feng-Qi(赵凤起), XU Si-Yu (徐司雨), et al. *Acta Phys.-Chim. Sin.* (*Wuli Huaxue Xuebao*), **2007**,**23**(9):1316~1320